ABERRANT GENE TRANSCRIPTIONAL ACTIVITY AS A FACTOR FOR RADIORESISTANCE OF HT-29 CELL LINEAGE

Kutilin D.S., Gusareva M.A., Kosheleva N.G., Gabrichidze P.N., Dontsov V.A., Legostaev V.M., Shlyakhova O.V., Liman N.A., Solntseva A .A., Krokhmal Yu.N.

National Medical Research Oncology Center of Russian Federation, Rostov-on-Don, e-mail: k.denees@yandex.ru

Aims

The objective of the study was screening for predictors of colorectal cancer radioresistance in a model experiment based on the data of aberrant expression of genes that regulate the system of signalling cascades involved in DNA repair, regulation of the cell cycle and apoptosis.

Materials and Methods

The study used human HT-29 cell culture. Transcription activity values were identified using the RT-qPCR method for 32 genes (*ATM, AKT, BRCA1, BRCA2, BRIP, CDK1, CDKN1B, CCND1, CCND3, FGFR2, HIST1, H2AX, KU70, EXO1, PTEN, RAD50, RAP80, RNF168, TOPB1, RIF1TP53, MDM2, XRCC4, BAX, BCL2, CASP8, CASP3, CASP9, RBBP8, EP300, LIG4, C-FLIP*).

Results

Statistically significant ($p<0.05$) increases in expression of *BRCA2, H2AX, CASP9* and *RBBP8* and decrease of expression of *BCL2* were registered in the cells exposed to the doses of 5 and 7 Gy as compared to the intact cells. A statistically significant ($p<0.05$) increase in expression of the *RIF1* gene was also registered in the cells exposed to irradiation with the dose of 7 Gy.

Conclusions

It was discovered in the course of the study that the *HT-29* cell line has an initially heterogeneous expression of a number of genes, and radiotherapy results in selective survival of a specific cell pool with a more potent DNA repair system (*BRCA2, H2AX*, and *RBBP8*) and a more efficient apoptosis regulation system (*CASP9, BCL2*).

Keywords: radiotherapy, colorectal cancer, cell culture, gene expression, apoptosis, DNA repair.

INTRODUCTION

Colorectal cancer (CRC) is the 4th most lethal cancer worldwide. In 2018 alone, it killed over 310,000 people [1].

Its high prevalence urges research and development of treatments for this nosology. Radiation therapy (RT) for CRC is important for symptom alleviation and local control of the disease. RT reduces the local recurrence rates and causes the tumor to shrink. However, a full clinical response is extremely rare. The key factor is the radioresistance of tumor cells. Although several markers have been suggested for use as chemotherapy and RT response predictors, none of them is in clinical use. Since CRC constitutes a heterogeneous group of diseases, a universal molecular predictive marker is hard to find. In vitro experiments using cell lines showed several genetic loci (*XRCC3, XRCC2, FGFR4*, and *NF-KB*) that could potentially determine the RT sensitivity; however, further research into tumor cell radioresistance is still needed [2, 3, 4].

The goal hereof was therefore to screen the CRC radioresistance predictors in a model experiment using data on the aberrant expression of genes regulating the signal cascades involved in DNA repair, cell cycle regulation, and apoptosis.

MATERIALS AND METHODS

The study used an HT-29 human cell culture. The COrDIS Sprint kit was used to genotype the cells to verify that they matched the genotype of this cell line and were not contaminated. Cells were cultured in sterile vials (RPMI-1640, 10% fetal bovine serum, 50 μg/ml of gentamicin) at 5% CO_2, 95% humidity, and 37 °C in a CB-150 CO_2 incubator [5].

For the model experiment, the cultures were irradiated five times every 24 hours using a Novalis TX linear accelerator (Varian, USA) at 5 and 7 Gy. A Somatom Definition AS Siemens tomograph was used for topometry [5].

Total cell count and the living/dead cell ratio were evaluated in a Goryaev chamber

using a 0.4% trypan blue solution. After the 5th exposure, the cell line was removed from the substrate of the sterile vial using the Trypsin-Versene solution. Apoptosis stage-specific cell counts were found using a FACSCanto II (BD, USA) cell analyzer and an Annexin V-FITC Apoptosis Detection Kit [5].

The HT-29 cell culture was cleansed of the medium with Dulbecco's phosphate-buffered saline and centrifugated; 900 µl of QIAzol (QIAGEN) was added to the sediment. Total RNA was further fractionated and purified using RNeasy Plus Universal Kits (QIAGEN) per the manufacturer's protocol. Ready RNA preparations were treated with DNase I to remove traces of genomic DNA. RNasin was added to the finished RNA preparation until reaching a concentration of 1 U/µl.

The quality of the resulting RNA was tested by agarose gel electrophoresis in terms of rRNA 28S/18S brightness, see Fig. 1.

The concentration of the obtained RNA preparations was measured by a Qubit 2.0® fluorometer (Invitrogen, USA).

For cDNA buildup, the research team prepared a reaction mixture containing 5 µM of random primers, 1x RT buffer, 0.5 µM of dNTP mix, 0.5 U/µl of RNase Inhibitor (Thermo scientific), 5 U/µl of Reverse Transcriptase MMLV (Sintol, Russia), and the isolated RNA as the matrix. The resulting mix was incubated at 44 °C for over 1 hour; the reverse transcriptase was inactivated at 92 °C for over 10 minutes.

Real-time quantitative polymerase chain reaction (RT-qPCR) was performed to find the transcriptional activities of 32 genetic loci (*ATM, AKT, BRCA1, BRCA2, BRIP, CDK1, CDKN1B, CCND1, CCND3, FGFR2, HIST1, H2AX, KU70, EXO1, PTEN, RAD50, RAP80, RNF168, TOPB1, RIF1TP53, MDM2, XRCC4, BAX, BCL2, CASP8, CASP3, CASP9, RBBP8, EP300, LIG4, C-FLIP*). The stability of the reference genes was assessed by the geNorm algorithm. *GAPDH, ACTB*, and *B2M* were used as reference genes. Specific oligonucleotide primers were designed by means of NCBI GenBank and Primer-BLAST, see Table 1 for the primer sequence.

Each locus was set in three procedural repetitions. A reaction mixture (1x PCR buffer, 1.5 mM of $MgCl_2$, 0.2 mM of dNTP, 500 nM of each primer, 0.05 U/µl of Taq-polymerase, and 10 ng of cDNA) was used for amplification. NTC and NRT samples were used for internal control. The resulting mixtures were amplified in a CFX thermocycler (Bio-Rad, USA) at 95 °C over 240 seconds; 40 cycles: 10 seconds at t = 95 °C, 30 seconds at 58 °C, and 30 seconds at 72°C.

The relative expression was calculated by the formula: $RE=2^{-\Delta\Delta Ct}$.

The results were normalized by three reference genes (*GAPDH, ACTB,* and *B2M)* and by the expression of the corresponding target genes in the control group samples; see the procedure below.

1. Normalization by the geometric mean of the reference loci:

2. $\Delta C(t) = C(t)_{target} - {}_{geometric\ mean}C(t)_{reference}$.

3. The arithmetic mean ΔC(t) calculated for each gene for the control group (the intact group) and the exposed group.

4. Normalization by the control (intact) group:

5. $\Delta\Delta C(t) = {}_{arithmetic\ mean}\Delta C(t)_{of\ the\ exposed\ group} - {}_{arithmetic\ mean}\Delta C(t)_{of\ the\ control\ group}$.

6. The final result (factor of difference): $2_{-\Delta\Delta C(t)}$.[6].

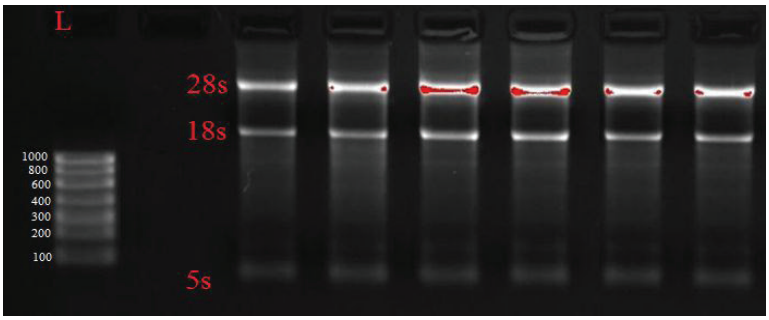

Fig. 1. Electrophoretic imaging of RNA isolated from freshly frozen rectal tumor tissue. Imaging performed with Gel Doc XR PLUS (BioRad, USA)

Table 1

Primer sequence for detecting relative gene expression

No.	Gene	5'→3' primer sequences
1	BRCA1	F: ACC TGT CTC CAC AAA GTG TGA
		R: ACA CTG TGA AGG CCC TTT CT
2	BRCA2	F: AGT TGG CTG ATG GTG GAT GG
		R: GGA TCC ACA CCT GGA GTG TC
3	PTEN	F: GGC ACA AGA GGC CCT AGA TA
		R: CTT AGC GCC TCT GAC TGG G
4	CASP3	F: CTG GAA TAT CCC TGG ACA ACA TT
		R: TCA ACA TCT GTA CCA GAC CGA
5	CASP8	F: CTG AAG CAA ACA GCC AGT GG
		R: GAT CTC AAT TCT GAT CTG CTC AC
6	GAPDH	F: GTC AAG GCT GAG AAC GGG AA
		R: TCG CCC CAC TTG ATT TTG GA
7	BAX	F: GGG ACG AAC TGG ACA GTA ACA
		R: GCT GCC ACT CGG AAA AAG AC
8	B2M	F: AGA TGA GTA TGC CTG CCG TG
		R: CTA TGA TGC TGC TTA CAT GTC TC
9	BCL2	F: GGA TCC AGG ATA ACG GAG GC
		R: GAA ATC AAA CAG AGG CCG CA
10	CASP9	F: TGA GAC CCT GGA CGA CAT CT
		R: TCC CTT TCA CCG AAA CAG CA
11	P53	F: TTG GAA CTC AAG GAT GCC CA
		R: CGG GAG GTA GAC TGA CCC T
12	MDM2	F: TAG GAG ATT TGT TTG GCG TGC
		R: CCT GCT GAT TGA CTA CTA CCA A
13	AKT1_V1	F: AGCTGGTGCATCAGAGGCTG
		R: TGTAGCCAATGAAGGTGCCA
14	ATM	F: TGCGTGGCTAACGGAGAAAA
		R: ATCACTGTCACTGCACTCGG
15	BRIP1	F: TTACCCGTCACAGCTTGCTA
		R: CTCATCTGCTGGTTTCCCACT
16	CDK1	F: AAGCCGGGATCTACCATACC
		R: CATGGCTACCACTTGACCTGT
17	CDKN1B	F: TAATTGGGGCTCCGGCTAAC
		R: GAAGAATCGTCGGTTGCAGGT
18	CCND1	F: GATCAAGTGTGACCCGGACT
		R: CTTGGGGTCCATGTTCTGCT
19	CCND3	F: GTGGAGACTGGCTCTGTTCG
		R: TCACATACCTCCTCGTCAGGT
20	FGFR2	F: AACAGTCATCCTGTGCCGAA
		R: TGGACTCAGCCGAAACTGTTA
21	KU70	F: ACGTAGAGGGCGTTGATTGG
		R: TGGCTACTGCTCACTTTGGC

No.	Gene	5'→3' primer sequences
22	RAD50	F: GCGTGCGGAGTTTTGGAATAG
		R: TTGAGCAACCTTGGGATCGT
23	RAP80	F: GAGTGAGCAGGAAGCTAGGG
		R: AGAAGGCCGGCAACTATTCA
24	EXO1	F: GAACAAGCCGGGGTTACAGA
		R: AGGAGGAAGCTTTTCAGAATTTTT
25	Rif1	F: GGCTGTTTCCATCGGTCACT
		R: CATACGACTGGTCAGAGTCAGG
26	RNF168	F: GCCAGTTCGTCTGCTCAGTA
		R: CTGCCGCCACCTTGCTTAT
27	HIST1	F: AAGAGCCTGGTAAGCAAGGG
		R: TGCACCCGTTGCCTTAGTTT
28	TopBP1	F: CCAACGAGTTCAGAAATGTCCAG
		R: AACGCCACTAAAAGGGTCACA
29	ACTB	F: AACCGCGAGAAGATGACCC
		R: AGCACAGCCTGG TAGCAAC
30	H2AX	F: GGCCTCCCAGGAGTACTAAGA
		R: CTCTTTCCATGAGGGCGGTG
31	XRCC4	F: TTGATCTGTGAAAGCGGGCG
		R: TCTCCATTTCTTAATACCTCTCCGT
32	RBBP8	F: CGAGGATTTGGCACTCTGGT
		R: ACAGGTCAAATACCGCCTCC
33	EP300	F: GCCCTCTACCTGACCCAAGT
		R: ATAGCCCATAGGCGGGTTG
34	LIG4	F: GGCTTGACGTCAGGAAACCAT
		R: GAAGTTTGTGAGGCAGCCAT
35	C-FLIP	F: GTGACAGCTGAGACAACAAGG
		R: TGGGGGAGTTCGTCCTGT

Note: F means 'forward primer', R means 'reverse primer'.

Data was processed statistically by one-way ANOVA in Statistica 8.0 (StatSoft Inc.). Author-written R scripts (R-Studio 8.10.173.987) were used for hierarchical clustering by Euclidean distance as well as for heat mapping. Edwards–Venn diagrams were plotted by an algorithm comparing multiple sets, which had been implemented in JavaScript. Gene clustering by function was performed using functional module detection (FMD). The Q value for each term linked to the functional modules was calculated using one-sided Fisher's exact test with Benjamini and Hochberg adjustment [7].

RESULTS

Ionizing radiation causes double-stranded DNA breaks in tumor cells; however, some tumor cell clones are able to boost the repair of such ruptures to overcome the cytotoxic effects of radiation; they can also boost other signaling pathways that are not part of the cell repair system [8].

In this model experiment, only one HT-29 cell pool remained viable. Thirty-two percent of cells remained viable after 5-Gy exposure, 20% did after 7-Gy exposure. This could be due to such cells' increased radioresistance resulting from specific molecular and genetic features. Irradiation of HT-29 cells returned the differential expression values of 32 genes in intact (control) and exposed cells, see Fig. 2.

Three main gene clusters were identified by the peculiarities of expression in intact and irradiated samples: **1** – *BRCA2,*

C-FLIP, CASP3, XRCC4, KU70, CDK1, **2** – *AKT, RBBP8, RAP80, EP300, BCL2, RAD50, FGFR2, H2AX, CCND3, CCND1,* and **3** – *TOPB1, ATM, RNF168 PTEN, BRIP, EXO1, BAX, TP53, CASP9, RIF1, CASP8, BRCA1, CDKN1B, HIST1, LIG4*.

The intact and irradiated cell groups can be clustered by the identity of gene expression, see Figures 2 and 3. Some genes of intact and irradiated cells are similar expression-wise at different clustering levels, see Figures 2 and 3, Table 2; this could be due to the fact the HT-29 line initially contained clones in which these genes reached a certain level of expression and thus enabled the selective survival of such clones.

Notably, four genes (*BRCA2*, *CASP9, H2AX, RBBP8*) had elevated expression in more than five of the tested groups; *BRCA2* expression was increased even in some intact cells, see Table 2.

Normalizing the relative expression in cells exposed to 5-Gy and 7-Gy radiation returned the following results: *RBBP8* expression increased by a factor of 1.7 and 2.2, *BRCA2* expression increased by a factor of 1.7 and 2.3, *H2AX* expression increased by a factor of 2.3 and 4.5, and *CASP9* expression increased by a factor 2.0 and 2.4, whilst *BCL2* decreased by a factor of 1.6 and 3.0 significantly at $p<0.05$ compared to cells. Cells exposed to 7 Gy of radiation also had a statistically significant increase in *RIF1* expression by a factor of 1.5 ($p<0.05$), see Fig. 4.

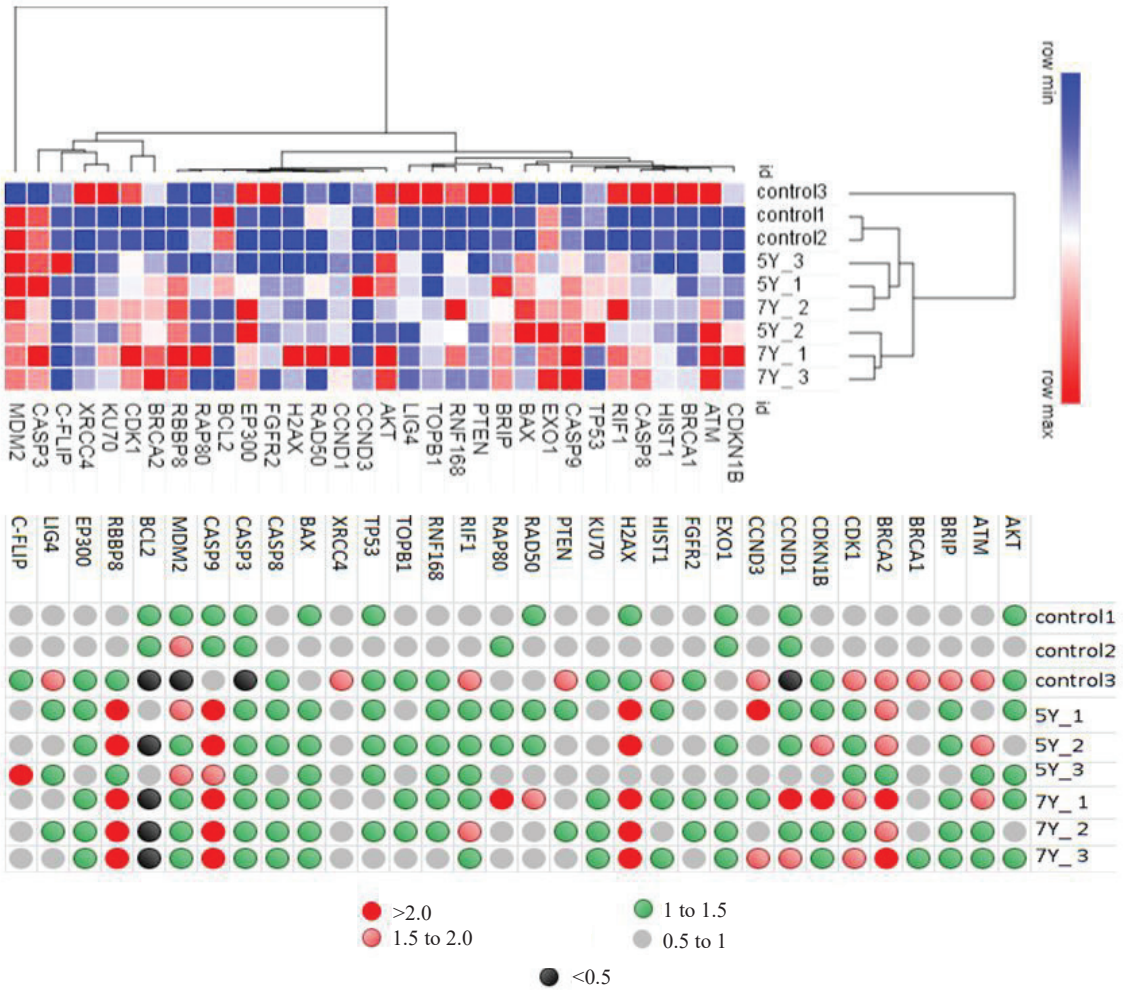

Fig. 2. Heatmap and cluster analysis of the differential expression of 32 genes in intact (control) and exposed HT-29 cells

Table 2

Similarities and differences between clusters in terms of gene expression

Gene	No. of higher-expression groups	Group name
BRCA2	6	control3, 5Y_1, 5Y_2, 7Y_1, 7Y_2, 7Y_3
CASP9	6	5Y_1, 5Y_2, 5Y_3, 7Y_1, 7Y_2, 7Y_3
H2AX	5	5Y_1, 5Y_2, 7Y_1, 7Y_2, 7Y_3
RBBP8	5	5Y_1, 5Y_2, 7Y_1, 7Y_2, 7Y_3
ATM	3	control3, 5Y_2, 7Y_1
CCND3	3	control3, 5Y_1, 7Y_3
CDK1	3	control3, 7Y_1, 7Y_3
MDM2	3	control2, 5Y_1, 5Y_3
CCND1	2	7Y_1, 7Y_3
CDKN1B	2	5Y_2, 7Y_2
RIF1	2	control3, 7Y_2

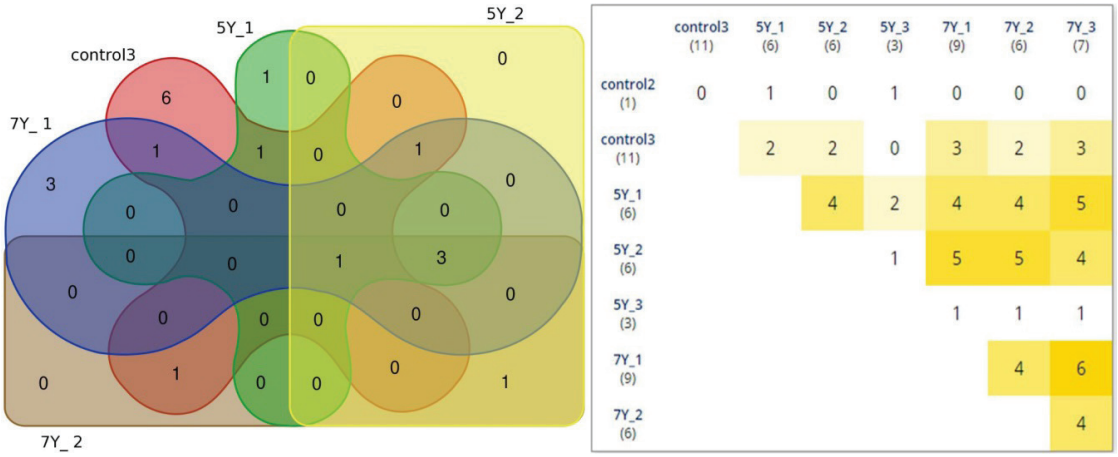

Fig. 3. Edwards-Venn diagram: similar numbers of high-expression genes in nine groups: three control groups, three 5-Gy groups, and three 7-Gy groups

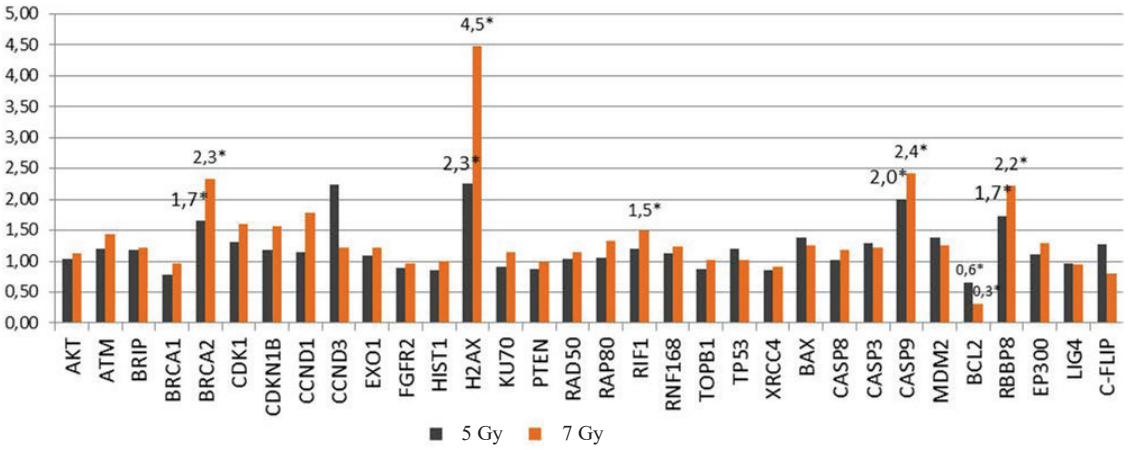

Fig. 4. Relative expression of genes in radioresistant HT-29 cells after 5-day exposure to 5-Gy and 7-Gy radiation
** statistically significant differences from the intact (control) cells ($p<0.05$)*

The FMD algorithm was applied to the tested genes (*ATM, AKT, BRCA1, BRCA2, BRIP, CDK1, CDKN1B, CCND1, CCND3, FGFR2, HIST1, H2AX, KU70, EXO1, PTEN, RAD50, RAP80, RNF168, TOPB1, RIF1TP53, MDM2, XRCC4, BAX, BCL2, CASP8, CASP3, CASP9,* c*RBBP8, EP300, LIG4, C-FLIP)* and split them into six functional modules, see Fig. 5 for visualization.

As shown in Fig. 5, a change in the expression of *BRCA2, CASP9,* and *RIF1* affects three functional modules in a group of signaling cell cascades: apoptosis regulation (M6, Q=0.0001), cellular response to irradiation (M4, Q<1e-4), and DNA repair (M1, Q<1e-4).

Multiple association network integration identified the interactions between the following genes: *BCL2, BRCA2, H2AX, CASP9, RBBP8, RIF1*, and *APAF1 (apoptotic peptidase activating factor 1), SPO11 (initiator of meiotic double stranded breaks), PALB2 (partner and localizer of BRCA2), APPL1 (adaptor protein, phosphotyrosine interacting with PH domain and leucine zipper 1), PSIP1 (PC4 and SFRS1 interacting protein 1), DIABLO (diablo IAP-binding mitochondrial protein), DMC1 (DNA meiotic recombinase 1) BIK, (BCL2 interacting killer), BAZ1B (bromodomain adjacent to the zinc finger domain 1B), FKBP8 (FK506 binding protein 8), BAG1 (BCL2-associated athanogene 1), RAD51, VDAC1 (voltage-dependent anion channel 1), XRCC3 (X-ray repair cross complementing 3), DCC (DCC netrin 1 receptor) RAD50 (RAD50 double-strand break repair protein), PSMC3IP (PSMC3 interacting protein), TEX15 (testis expressed 15), MND1 (meiotic nuclear divisions 1), and AIFM1 (apoptosis inducing factor, mitochondria associated 1)*, see Fig. 6. The algorithm predicts the function of a gene in a complex multigene network by applying a machine learning method based on the Gaussian field label distribution. The algorithm assigns the computed association strength to each node in the constructed network [9]. Thus, *BRCA2, H2AX, BCL2, CASP9, and RBBP8* are components of different signaling pathways in tumor cells; changing their transcriptional activity will modulate the activity of multiple other genes, see Fig. 6.

As ionizing radiation causes a double-stranded DNA break, H2AX (a histone protein coded by the *H2AX* gene) becomes serine-phosphorylated (γH2AX). This decondenses the DNA and frees up space for the attachment of protein complexes such as MRN (Mre11, Rad50, and Nbs1), RAD51, and ATM that are necessary for DNA repair [10, 11].

The *BRCA2*-encoded protein is also necessary for post-exposure DNA repair as it interfaces directly with recombinase RAD51, thus stimulating an important stage of homologous recombination [12]. *RBBP8* encodes a protein that regulates cell proliferation [13]. Accordingly, increased *BRCA2, H2A*, and *RBBP8* expression in some of the HT-29 clones likely made DNA repair more efficient, which gave these cells an advantage and enabled them to survive radiation.

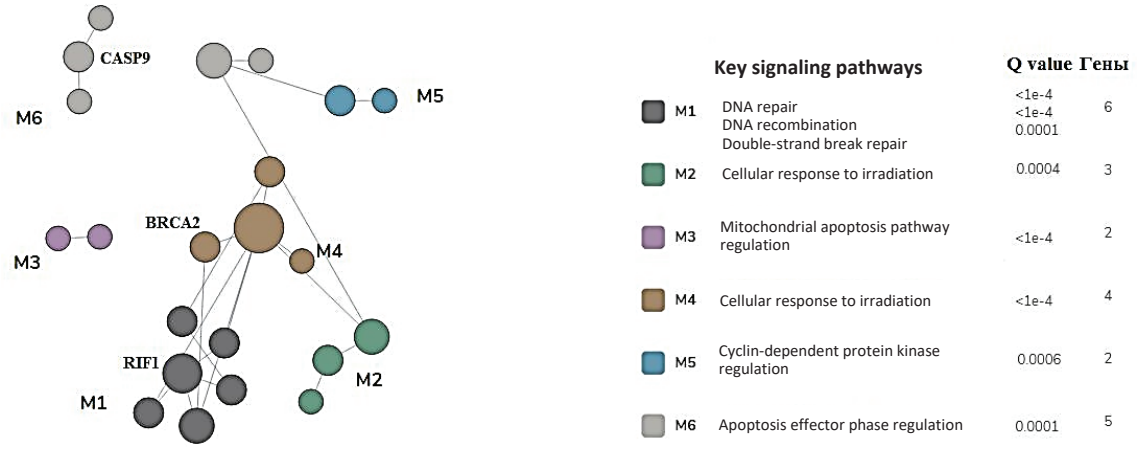

Fig. 5. Functional classification of the signaling pathways including 32 genetic loci

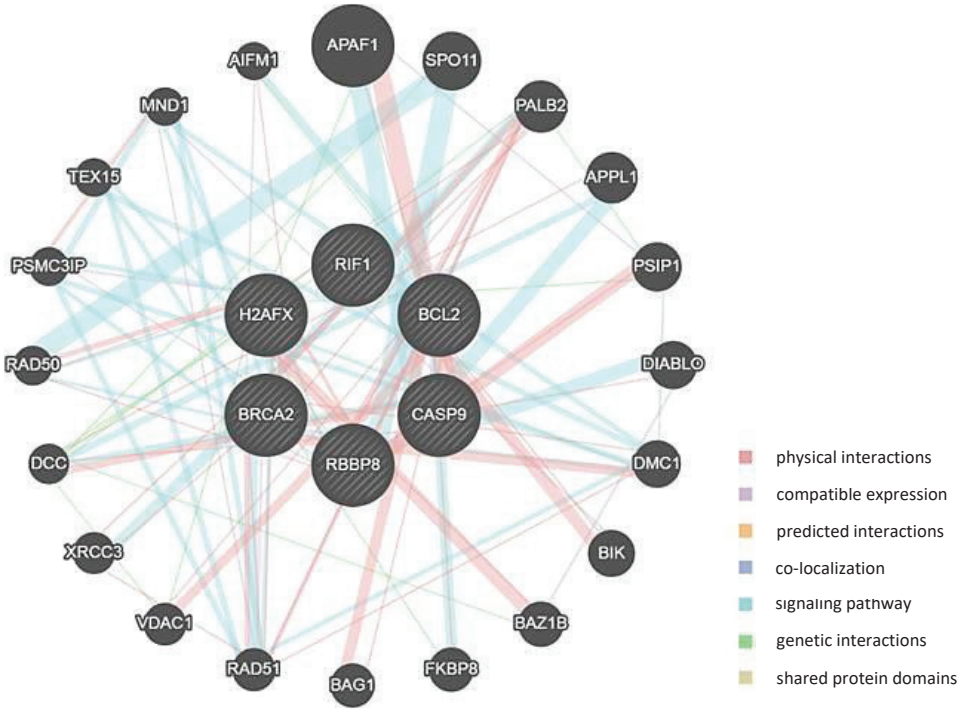

Fig. 6. Gene interactions computed by the multiple association network integration algorithm

BCL2 and CASP9 are two proteins important for the regulation of apoptosis. BCL2 suppresses apoptosis by altering the permeability of the mitochondrial membrane, which prevents the release of cytochrome C from mitochondria and inhibits caspases (inhibition is also implemented by binding APAF1, an apoptosis-activating factor). On the contrary, caspase-9 is a critical apoptosis-initiating protein that APAF1 activates by splicing pro-caspase-9 [14]. Accordingly, an increased *CASP9* expression coupled with reduced *BCL2* expression may lead to more efficient apoptosis compared to intact cells. It can be assumed this trait may somewhat regulate the population of HT-29 clones that have these molecular and genetic features.

CONCLUSIONS

Thus, this study has identified the original heterogeneity of HT-29 cells in terms of the transcriptional activity of some repair- and apoptosis-regulating genes. This heterogeneity is fundamental to the selective cell survival past 5-Gy and 7-Gy irradiation: the survivors had a more efficient DNA repair system with a higher transcriptional activity of BRCA2, H2AX, and RBBP8, and a more efficient apoptosis regulation system with a more transcription-active proapoptotic CASP9 gene and a less transcription-active anti-apoptotic BCL2 gene.

FINANCIAL SUPPORT AND SPONSORSHIP

The research was carried out as part of the Government Contract: Search for Rectal Cancer Radioresistance Predictors and Development of Personified Neoadjuvant Therapeutic Approaches

CONFLICTS OF INTEREST

The authors declare no conflict of interest

REFERENCES

1. Bray F., Ferlay J., Soerjomataram I. et al. Global cancer statistics 2018: GLOBOCAN estimates of incidence and mortality worldwide for 36 cancers in 185 countries. CA: A Cancer Journal for Clinicians. 2018, vol. 68, no. 6, pp. 394-424, doi: 10.3322/caac.21492.

2. Agostini M., Zangrando A., Pastrello C. et al. A functional biological network centered on XRCC3: a new possible marker of chemoradiotherapy resistance in rectal cancer patients. *Cancer Biology & Therapy*. 2015, vol. 16, no 8, pp. 1160-1171, doi 10.1080/15384047.2015.1046652.

3. Qin C.J., Song X.M., Chen Z.H. et al. XRCC2 as a predictive biomarker for radioresistance in locally advanced rectal cancer patients undergoing preoperative radiotherapy. *Oncotarget*. 2015, vol. 6, no. 31, pp. 32193-32204, doi 10.18632/oncotarget.4975.

4. Voboril R., Rychterova V., Voborilova J. et al. NF-κB/p65 expression before and after treatment in rectal cancer patients undergoing neoadjuvant (chemo) radiotherapy and surgery: prognostic marker for disease progression and survival. *Neoplasma*. 2016, vol. 63, no. 3, pp.462-470, doi 10.4149/317_151013n525.

5. Kutilin D.S., Kosheleva N.G., Maksimov A.Iu. et al. Effects of various radiotherapy doses on survival of colon adenocarcinoma cells line HT-29. [Vliianie razlichnykh doz luchevoi terapii na vyzhivaemost' kletok adenokartsinomy tolstoi kishki linii HT-29]. *Modern problems of science and education - Sovremennye problemy nauki i obrazovaniia.* 2019, no 3, available at: http://science-education.ru/ru/article/view?id=28918, (accessed 15.07.2020), doi: 10.17513/spno.28918.

6. Kutilin D.S., Mogushkova Kh.A. The effect of anthracycline antitumor antibiotics on the transcription of cancer-testis antigens in the model experiment on HeLa cell line [Vliianie protivoopukholevykh antibiotikov antratsiklinovogo riada na transkriptsionnuiu aktivnost' rakovo-testikuliarnykh antigenov v model'nom eksperimente na kletochnoi linii HeLa]. *Medical Immunology - Meditsinskaia immunologiia*, 2019, vol. 21, no. 3, pp. 539-549.

7. Krishnan A., Zhang R., Yao V. et al. Genome-wide prediction and functional characterization of the genetic basis of autism spectrum disorder. *Nature Neuroscience*. 2016, vol. 19, no. 11, pp. 1454- 1462, doi 10.1038/nn.4353.

8. Weichselbaum R.R., Liang H., Deng L. et al. Radiotherapy and immunotherapy: a beneficial liaison? *Nature Reviews Clinical Oncology*, 2017, vol. 14, no. 6, pp. 365-379, doi 10.1038/nrclinonc.2016.211.

9. Warde-Farley D., Donaldson S.L., Comes O. et al. The GeneMANIA prediction server: biological network integration for gene prioritization and predicting gene function. *Nucleic Acids Research*. 2010, vol. 38, no. 2, pp. 214-220, doi 10.1093/nar/gkq537.

10. Ayoub N., Jeyasekharan A.D., Bernal J.A. et al. HP1-β mobilization promotes chromatin changes that initiate the DNA damage response. *Nature*. 2008, vol. 453, no. 7195, pp. 682-686, doi 10.1038/nature06875.

11. Bekker-Jensen S., Lukas C., Kitagawa R. et al. Spatial organization of the mammalian genome surveillance machinery in response to DNA strand breaks. *Journal of Cell Biology*. 2006, vol. 173, no. 2, pp. 195-206, doi 10.1083/jcb.200510130.

12. Wang C.X., Jimenez-Sainz J., Jensen R.B. et al. The Post-Synaptic Function of Brca2. *Scientific Reports*. 2019, vol. 9, no. 1, doi 10.1038/s41598-019-41054-y.

13. Sartori A.A., Lukas C., Coates J. et al. Human CtIP promotes DNA end resection. *Nature*. 2007, vol. 450, no 7169, pp. 509-514, doi 10.1038/nature06337.

14. Kutilin D.S., Kosheleva N.G., Gusareva M.A et al. Gene copy number variation as a factor of radioresistance of colon adenocarcinoma cells of the line HT-29. [Kopiinost' genov kak faktor radiorezistentnosti kletok adenokartsinomy tolstoi kishki linii HT-29]. *Modern problems of science and education - Sovremennye problemy nauki i obrazovaniia.* 2019, no 5, available at: http://science-education.ru/ru/article/view?id=29224, (accessed 15.07.2020), doi: 10.17513/spno.29224.